Anomalous angular dependence of the upper critical induction of orthorhombic ferromagnetic superconductors with completely broken *p*-wave symmetry

Christopher Lörscher,[1] Jingchuan Zhang,[1,2] Qiang Gu,[2] and Richard A. Klemm[1]

[1]*Department of Physics, University of Central Florida, Orlando, FL 32816-2385 USA*
[2]*Department of Physics, University of Science and Technology Beijing, Beijing 100083, China*

(Dated: October 30, 2012)

We calculate the upper critical induction $B_{c2}(\theta,\phi)$ of an orthorhombic ferromagnetic superconductor with parallel-spin p-wave pairing along $\hat{\boldsymbol{e}}_3$ and an ellipsoidal Fermi surface with effective masses m_1, m_2, and m_3, where $\hat{\boldsymbol{B}}\cdot\hat{\boldsymbol{e}}_3 = \cos\theta$. At fixed θ, an ordinary $B_{c2}(\phi)$ is obtained, but at fixed ϕ, a novel $B_{c2}(\theta)$ is predicted. For fixed $3 < m_3/(m_1\cos^2\phi + m_2\sin^2\phi)$, an anomalous peak in B_{c2} occurs at $0^\circ < \theta^* < 90^\circ$, providing a sensitive bulk test of the order parameter orbital symmetry in both phases of clean URhGe samples. The method is generalizable to any order parameter.

Recent discoveries of materials with coexistent superconductivity and ferromagnetism spawned renewed interest in parallel-spin triplet superconductivity, the simplest cases having p-wave orbital symmetry [1–11]. In a non-cubic crystal structure, there can be a variety of different p-wave states present, which can be characterized by measurements of the temperature T dependence of the upper critical induction B_{c2} [12–18]. Ambient pressure measurements of the ferromagnetic superconductors UCoGe [1, 2] and URhGe [3–7] showed that the superconductivity exists completely within the ferromagnetic T range and that the same electrons are responsible for the superconductivity and the ferromagnetism[2].

In URhGe, B_{c2} measurements in the low-field regime on a sample with room temperature resistivity ratio (RRR) = 21 were fit to the Scharnberg-Klemm theory of the crystal-aligned p-wave polar state of completely broken symmetry (CBS), using the three resistively-measured slopes of B_{c2} just below the ferromagnetic demagnetization jumps at T_c as the only fitting parameters [4]. The measured $B_{c2,a}(T)$ fit the predicted behavior for the polar state, and both $B_{c2,b}(T)$ and $B_{c2,c}(T)$ fit the qualitatively different predicted curve for the CBS state, with a constant ratio $B_{c2,b}(T)/B_{c2,c}(T)$ due apparently to T-independent "effective mass" anisotropy. In addition, even in the low-field superconducting regime, in all three crystal directions, H_{c2} strongly violated the Pauli limit $H_p \sim 1.85T_c$ (K) for a singlet-spin s-wave superconductor[4], further suggesting a parallel-spin pair state coexisting with the ferromagnetic state. Together, the data provided strong evidence that the superconducting order parameter is likely to have the simplest parallel-spin p-wave orbital form consistent with ferromagnetism in the bc plane of an orthorhombic crystal, $\hat{\boldsymbol{d}}k_a$, where the pair-spin $\hat{\boldsymbol{d}} = (\hat{\boldsymbol{b}} + i\hat{\boldsymbol{c}})/\sqrt{2}$, with the p-wave pairing interaction fixed to the crystal a-axis direction for all magnetization $\boldsymbol{M} \perp \hat{\boldsymbol{a}}$ directions and the two parallel-spin states indicated by $\hat{\boldsymbol{b}} = |\uparrow\uparrow\rangle$ and $\hat{\boldsymbol{c}} = |\downarrow\downarrow\rangle$ [8].

Subsequent measurements on a URhGe sample with RRR = 50 [5] observed an anomalous high magnetic field $\boldsymbol{H}$ reentrant superconducting phase for $\boldsymbol{H}||\hat{\boldsymbol{b}}$ [5], which was associated with a first-order metamagnetic transition and a topological Fermi surface Lifshitz transition [6, 7]. But the angular dependence of B_{c2} within the ab plane in the low-field regime was found to be consistent with that of an ordinary superconductor with just effective mass anisotropy, at least within the relatively low resolution of the experiment designed for operation at much higher magnetic fields $\boldsymbol{H}$ [5]. At first sight, these results appear to be in contradiction with the earlier measurements of B_{c2} in URhGe [4].

In this letter, we address this issue by calculating the full (θ,ϕ) dependencies of B_{c2} for the candidate p-wave polar/CBS state. We calculate the θ dependencies within the ab-plane for the RRR = 21 and 50 crystals, and predict that under some conditions, URhGe could exhibit a non-monotonic $B_{c2}(\theta,\phi)$ curve with a peak at $0^\circ < \theta^* < 90^\circ$ at fixed ϕ, providing a definitive bulk test of the orbital symmetry of the order parameter. Our method is applicable to all superconductors.

Since T_c in ferromagnetic superconductors such as URhGe is relatively low, we assume weak coupling for a clean homogeneous type-II parallel-spin p-wave superconductor with effective Hamiltonian [12, 13],

$$\hat{H} = \sum_{i=1}^{3}\frac{1}{2m_i}\sum_{\boldsymbol{k}\sigma} a^\dagger_{\boldsymbol{k}\sigma}\left(p_i - eA_i\right)^2 a_{\boldsymbol{k}\sigma} + \frac{1}{2}\sum_{\boldsymbol{k},\boldsymbol{k}'\sigma} a^\dagger_{\boldsymbol{k}'\sigma}a^\dagger_{\boldsymbol{k}\sigma}V_{\sigma\sigma}(\hat{\boldsymbol{k}},\hat{\boldsymbol{k}}')a_{\boldsymbol{k}\sigma}a_{\boldsymbol{k}'\sigma}, \quad (1)$$

$$V_{\sigma\sigma'}(\hat{\boldsymbol{k}},\hat{\boldsymbol{k}}') = 3V_0\hat{\boldsymbol{k}}_a\hat{\boldsymbol{k}}'_a\hat{\boldsymbol{d}}\cdot\hat{\boldsymbol{d}}^* = 3V_0\hat{\boldsymbol{k}}_a\hat{\boldsymbol{k}}'_a, \quad (2)$$

where $\boldsymbol{p} = \hbar\boldsymbol{k}$, $\hat{k}_a \equiv \hat{\boldsymbol{k}}\cdot\hat{\boldsymbol{a}}$, the orbital symmetry of the equal-spin pairing interaction is that of a p wave locked onto the orthorhombic crystal lattice $\hat{\boldsymbol{a}} \equiv \hat{\boldsymbol{e}}_3$ direction, and the spins indexed by σ are quantized along the direction of $\boldsymbol{B} = \mu_0\boldsymbol{H} + \boldsymbol{M} = \boldsymbol{\nabla}\times\boldsymbol{A} = B\left(\sin\theta\cos\phi, \sin\theta\sin\phi, \cos\theta\right)$. This model includes the spontaneous magnetization $\boldsymbol{M}_0$ of the ferromagnetic superconductor, which produced only a minor jump in B_{c2} near to T_c in orthorhombic URhGe [4]. Here we assume an ellipsoidal Fermi surface with single-particle effective

masses m_i along the orthogonal $\hat{\boldsymbol{e}}_i$ directions, respectively. These m_i are generally different from anisotropic Ginzburg-Landau (AGL) effective masses [19].

The Maxwell equation-preserving Klemm-Clem transformations [19, 20] are exact at B_{c2} in the AGL model, and were subsequently applied to a microscopic calculation of B_{c2} in d-wave superconductors with $m_1 = m_2 < m_3$ [21]. Here the transformations allow us to calculate the effects of a general ellipsoidal Fermi surface on B_{c2} for a p-wave superconductor in the polar/CBS state, for which the order parameter anisotropy has a much stronger effect upon $B_{c2}(\theta,\phi)$ than in those d-wave cases.

Here the anisotropic-scale transformation changes the Fermi surface shape from ellipsoidal to spherical [20, 21], allowing us to employ the Feynman technique used to calculate $B_{c2}(T)$ for an isotropic s-wave superconductor neglecting Pauli limiting [22]. We set $p_i = p_i'\sqrt{\overline{m}_i}$, $A_i = A_i'\sqrt{\overline{m}_i}$, $x_i = x_i'/\sqrt{\overline{m}_i}$, and $B_i = B_i'/\sqrt{\overline{m}_i}$, where $\overline{m}_i = m_i/\left(m_1 m_2 m_3\right)^{1/3}$. This transformation changes $\boldsymbol{B}$ to $B'\left(\sin\theta'\cos\phi', \sin\theta'\sin\phi', \cos\theta'\right)$, where $\sin\phi' = (\overline{m}_2)^{1/2}\sin\phi/\overline{m}_{12}(\phi)$, $\sin\theta' = [\overline{m}_{12}(\phi)]^{1/2}\sin\theta/\alpha(\theta,\phi)$, $\overline{m}_{12}(\phi) = \overline{m}_1\cos^2\phi + \overline{m}_2\sin^2\phi$, $\alpha(\theta,\phi) = \left[\overline{m}_{12}(\phi)\sin^2\theta + \overline{m}_3\cos^2\theta\right]^{1/2}$, *etc.* [19, 20]

Next, we rotate the scaled coordinates so that the rotated induction $\boldsymbol{B}''$ points along the original pairing $\hat{\boldsymbol{e}}_3''$ direction. Finally, we make an isotropic scale transformation by $1/\alpha(\theta,\phi)$ [19, 20]. The transformations have two overall effects: First, $B \to B\alpha(\theta,\phi)$, modifying the slope of b_{c2} at T_c, even for an s-wave superconductor [19–23]. Second, the rotation modifies $V_{\sigma\sigma}(\hat{\boldsymbol{k}}, \hat{\boldsymbol{k}}')$ to

$$V_{\sigma\sigma}(\hat{\hat{\boldsymbol{k}}}, \hat{\hat{\boldsymbol{k}}}') = 3V_0(\hat{\hat{\boldsymbol{k}}}_3\cos\theta' - \hat{\hat{\boldsymbol{k}}}_2\sin\theta') \times(\hat{\hat{\boldsymbol{k}}}_3'\cos\theta' - \hat{\hat{\boldsymbol{k}}}_2'\sin\theta'), \quad (3)$$

which differently alters $b_{c2}(\theta,\phi,t)$ from that of its slope at T_c. We insert this rotated interaction into the linearized Gor'kov gap equation [20], project out the order parameter component, expand it in terms of the vortex harmonic oscillator states [12, 13], and obtain a general recursion relation for the expansion coefficients a_n, $\Gamma_n a_n = \frac{1}{2}\sin^2\theta'(\beta_n a_{n+2} + \beta_{n-2}a_{n-2})$, where

$$\Gamma_n = -\ln t + \cos^2\theta'\alpha_n^{(p)} + \sin^2\theta'\alpha_n^{(a)}, \quad (4)$$

$$\alpha_n^{(p,a)} = \pi T\sum_{\omega_n}\int_0^\pi d\theta_k \sin\theta_k \begin{pmatrix} 3\cos^2\theta_k \\ \frac{3}{2}\sin^2\theta_k \end{pmatrix} \times\int_0^\infty d\xi e^{-2\xi|\omega_n|}e^{-\eta/2}L_n(\eta), \quad (5)$$

$$\beta_n = \pi T\sum_{\omega_n}\int_0^\pi d\theta_k\frac{3}{2}\sin^3\theta_k\int_0^\infty d\xi e^{-2\xi|\omega_n|} \times e^{-\eta/2}\sum_{p=0}^{n}\frac{(-\eta)^{p+1}\sqrt{(n+1)(n+2)}n!}{p!(p+2)!(n-p)!}, \quad (6)$$

$t = T/T_c$, $T_c = (2\gamma\omega_0/\pi)\exp\left(-1/N(0)V_0\right)$, $N(0)$ is the density of states per spin at the Fermi energy, ω_0 is a characteristic pairing cutoff frequency, $\gamma \approx 1.781$ is the exponential of Euler's constant, $L_n(z)$ are the Laguerre polynomials, and $\eta = eB\xi^2 v_F^2\sin^2\theta_k\alpha(\theta,\phi)$. Equations (4-6) differ from those in Refs. [12,13] only in the general θ' in Eq. (4) and in the factor $\alpha(\theta,\phi)$ in η. From the recursion relation above Eq. (4), $B_{c2}(\theta,\phi,t)$ is implicitly obtained from the continued-fraction equation,

$$\Gamma_0 - \frac{\frac{1}{4}\sin^4\theta'\beta_0^2}{\Gamma_2 - \frac{\frac{1}{4}\sin^4\theta'\beta_2^2}{\Gamma_4\cdots}} = 0. \quad (7)$$

Usually, 4 or 5 iterations yield sufficient accuracy.

In Fig. 1 (a), we assumed a spherical Fermi surface and plotted the reduced induction $b_{c2} = 2eB_{c2}v_F^2/(2\pi T_c)^2$ versus t for θ values increasing from 0° to 90° from top to bottom in increments of 10°. $b_{c2}(0°,t)$ and $b_{c2}(90°,t)$ are those of the polar and CBS states [13]. $b_{c2}(\theta,t)$ decreases monotonically with increasing θ, but is less sensitive to θ for $\theta \sim 0°$ and especially for $\theta \sim 90°$ than in the case of ordinary effective mass anisotropy. As θ increases from 0° to 90°, $-db_{c2}(\theta,t)/dt|_{t=1}$ decreases monotonically by an overall factor of $1/\sqrt{3}$. Since this slope variation is indistinguishable from that which could arise from effective mass anisotropy, the same curves are rescaled by $-db_{c2}/dt|_{t=1}$ in Fig. 1(b). Order parameter anisotropy effects are easiest to identify for $t \ll 1$. [13, 14].

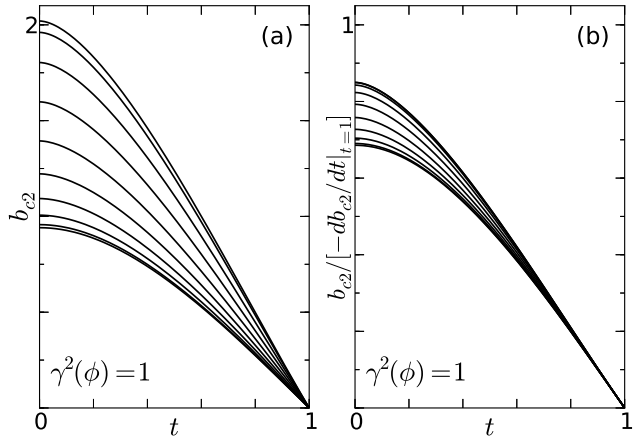

FIG. 1: (a) Plots of $b_{c2}(\theta,t) = 2eB_{c2}v_F^2/(2\pi T_c)^2$ for a spherical Fermi surface with θ increasing from 0° (top, polar state) to 90° (bottom, CBS state) in increments of 10°. (b) The same curves in Fig. 1(a) curves normalized by $-db_{c2}/dt|_{t=1}$.

At fixed t, $b_{c2}(\theta,\phi,t)$ for a polar/CBS p-wave superconductor with a general ellipsoidal Fermi surface only depends upon $\alpha(\theta,\phi)$ and $\sin^2\theta'$, $b_{c2}(\pi-\theta,\phi,t) = b_{c2}(\theta,\phi,t)$, the entire ϕ dependence of b_{c2} can be incorporated into the Fermi surface anisotropy function [19, 20]

$$\gamma^2(\phi) = m_3/m_{12}(\phi), \quad (8)$$

and $-db_{c2}(\theta,\phi,t)/dt\big|_{t=1} \propto [3\sin^2\theta/\gamma^2(\phi) + \cos^2\theta]^{-1/2}$ [13], suggesting $\gamma^2(\phi) = 3$ signals a crossover from order parameter to Fermi surface anisotropy as $t \to 1-$.

In Fig. 2, we plotted $b_{c2}(\theta,t)/b_{c2}(0,t)$ for a variety of fixed $\gamma^2(\phi)$ values at $t = 0, \frac{1}{2}$. At lower t and as $\gamma^2(\phi)$ increases from 0.1 to 3, there is an increasing difference between $b_{c2}(\theta,t)$ and the effective anisotropic mass form,

$$b_{c2}^{\rm eff}(\theta) \;=\; \left[\cos^2\theta/b_{c2}^2(0^\circ) + \sin^2\theta/b_{c2}^2(90^\circ)\right]^{-1/2} \quad (9)$$

fitted at each t. For fixed $\gamma^2(\phi)$ increasing above 3, an anomalous peak at $0^\circ < \theta^* < 90^\circ$ is clearly evident at $t = 0$ and in the 3.7 and 5.9 curves at $t = \frac{1}{2}$. For $\gamma^2(\phi) = 10$, $b_{c2}(\theta, \frac{1}{2})$ only has a conventional maximum at $\theta = 90^\circ$. The anomalous non-monotonicity is due to competing order parameter and Fermi surface anisotropy effects.

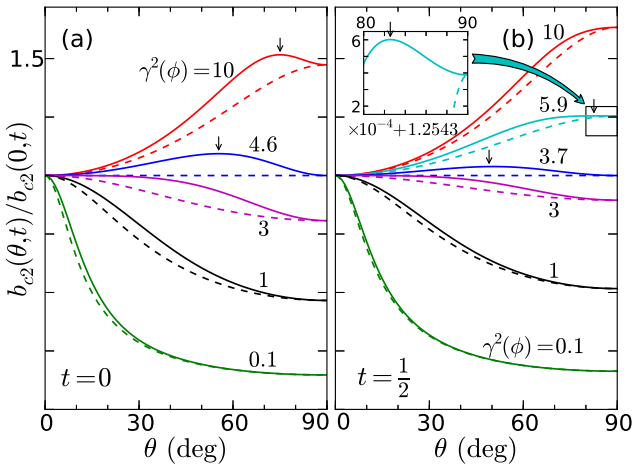

FIG. 2: (color online) Calculated $b_{c2}(\theta,t)/b_{c2}(0,t)$ (solid) and fitted $b_{c2}^{\rm eff}(\theta,t)/b_{c2}(0,0)$, Eq. (9), (dashed) curves at constant $\gamma^2(\phi)$ values. The arrows indicate peak maxima at θ^* points. (a) $t = 0$ (b) $t = 1/2$. The inset is an enlargement of the $80^\circ \le \theta \le 90^\circ$ region of the $\gamma^2(\phi) = 5.9$ curves, with the indicated vertical scale points 1.2545 and 1.2549.

We calculated the Fermi surface effective masses from the RRR = 21 URhGe crystal data [4]. In Fig. 3(a) we present the calculated $b_{c2}(\theta,t)/b_{c2}(0,0)$ in the ab plane (with $\boldsymbol{B} \perp \hat{\boldsymbol{c}}$) for different t values as functions of θ. The dashed lines represent fits to the corresponding fitted curve using Eq. (9). For low t, the order parameter anisotropy plays an integral role in the anisotropy of b_{c2}, while for $t \sim 1$, order parameter anisotropy is very small. Since the Fermi surface effective mass anisotropy is weaker in the ab plane than in the ac plane, our results differ substantially in this plane from those of Eq. (9). As noted above, in the bc plane ($\theta = \pi/2$), $b_{c2}(\phi) \propto \gamma(\phi)$. This is consistent with their data, since their b and c-axis data were both fit to the $b_{c2}(t)$ of the CBS state [4].

We also performed similar calculations to make predictions for $b_{c2}(\theta,\phi,t)$ in the RRR = 50 URhGe sample [5].

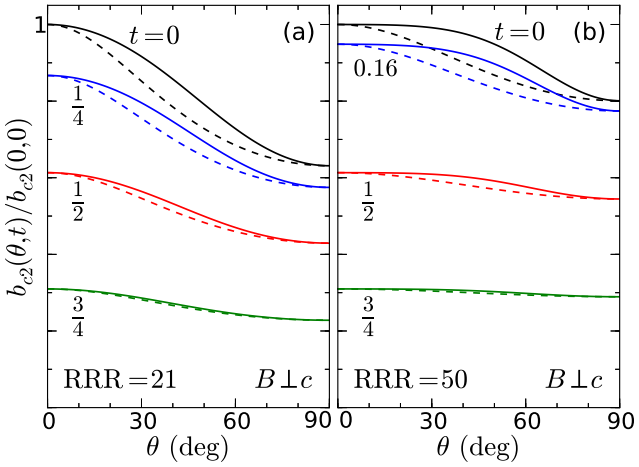

FIG. 3: (color online) Calculated $b_{c2}(\theta,t)/b_{c2}(0,0)$ (solid) and fitted $b_{c2}^{\rm eff}(\theta,t)/b_{c2}(0,0)$, Eq. (9), (dashed) curves for $\boldsymbol{B} \perp \hat{\boldsymbol{c}}$ at various t values for the Fermi surface effective mass values obtained from experiment. (a) URhGe sample with RRR = 21 [4]. (b) URhGe sample with RRR = 50 [5].

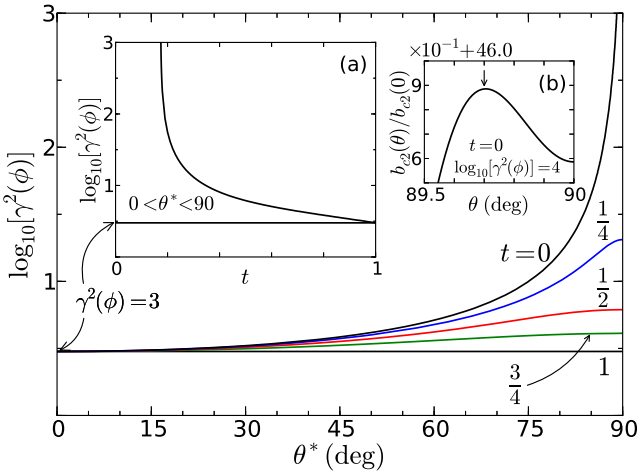

FIG. 4: (color online) Logarithmic plot of $\gamma^2(\phi)$ as a function of θ^*, the peak angle in $b_{c2}(\theta,t)$, at the indicated t values. Inset (a): Plot of the $0 < \theta^* < 90^\circ$ region versus $\log_{10}[\gamma^2(\phi)]$ and t. Inset (b): Plot of $b_{c2}(\theta,0)/b_{c2}(0,0)$ versus θ near to θ^* for $\gamma^2(\phi) = 10^4$. The vertical scale runs from 46.5 to 47.

In Fig. 3(b), the calculated $b_{c2}(\theta,t)/b_{c2}(0,0)$ and correspondingly fitted curves are plotted in the ab plane as a function of θ for various t, including $t = 0.16$, the lowest measurement value [5]. From subsequent Shubnikov-de Haas measurements [6], a strong $\boldsymbol{B}||\hat{\boldsymbol{b}}$ appears to increase the pairing interaction strength V_0 and decrease the relevant effective Fermi velocity [6] of the heavy-electron ellipsoidal Fermi surface responsible for the pairing [9–11]. By rotating a strong $\boldsymbol{B}$ a limited ϕ range in the bc plane, they concluded that the cyclotron mass $m^* = \sqrt{m_{12}(90^\circ+\phi)m_3}$ of the small spin-aligned heavy-

electron Fermi surface was independent of ϕ. Although they could not determine γ^2 without rotating $\boldsymbol{B}$ outside the bc plane, they provided strong justification for an ellipsoidal Fermi surface, and indicated that the Fermi wave vector k_F decreases dramatically with increasing B, vanishing at 15.5 T, at which a topological Lifshitz transition occurs [6]. We note that b_{c2} and h_{c2} differ greatly for these field strengths due to the large $\boldsymbol{M}_0||\hat{\boldsymbol{c}}$ [7]. More important, if the order parameter in the reentrant phase maintains the polar/CBS form [8], dramatic further increases in V_0 and potentially in $\gamma^2(\phi)$ would be expected as the metamagnetic transition is approached [6], and the angle between $\boldsymbol{B}$ and $\boldsymbol{H}$ would decrease dramatically [7], yielding an observable anomalous peak in $b_{c2}(\theta, t)$ as depicted in Fig. 2. We propose that further measurements of $h_{c2}(\theta, t \ll 1)$ be made in the low-field and especially in the reentrant phase of URhGe, in which $\hat{\boldsymbol{M}}$ changes rapidly from $\hat{\boldsymbol{c}}$ to $\hat{\boldsymbol{b}}$, as this could provide a definitive identification of the symmetry of the order parameter and further support to a ferromagnetic mechanism for superconductivity in both phases of URhGe.

In Fig. 4, we plotted $\log_{10}[\gamma^2(\phi)]$ versus θ^*, the anomalous peak angle in $b_{c2}(\theta, 0)$. Anomalous peaks appear for $\gamma^2(\phi) > 3$ and disappear for $\gamma^2(\phi) < \lambda(t)$, where $\lambda(t)$ increases very rapidly with decreasing t for $t < 0.15$, as shown in inset (a). Inset (b) details the anomalous peak in $b_{c2}(\theta, 0)$ for $\gamma^2(\phi) = 10^4$.

Conventional peaks in $b_{c2}^{\rm eff}(\theta)$ occur only at either $\theta = 0^\circ$ or $\theta = 90^\circ$, but anomalous peaks only occur for $0 < \theta^* < 90^\circ$. However, since $b_{c2}(\theta, \phi, t) = b_{c2}(180^\circ - \theta, \phi, t)$, a second anomalous peak at $180^\circ - \theta^*$ is reflection-symmetric in shape about 90° to that of the first one. When θ^* is close to 90°, the magnitude of each anomalous peak is very small, but accurate measurements of this double peak could provide a definitive bulk test of the orbital symmetry of the order parameter.

Ellipsoidal Fermi surface anisotropy can be included in accurate calculations of $B_{c2}(\theta, \phi, t)$ for superconductors of any orbital order parameter symmetry. If Sr_2RuO_4 were a chiral $p_x \pm ip_y$ state as purported [24], $B_{c2}(\theta, t)$ would be that of an SK state fixed to the xy plane [12], although $B_{c2}(90^\circ, 0)$ appears Pauli-limited [19, 25, 26]. An approximation of our procedure was employed to fit the extremely Pauli-limited in-plane $B_{c2}(90^\circ, \phi, t \ll 1)$ of $CeCu_2Si_2$ [27]. An accurate calculation of $B_{c2}(\theta, \phi, t)$ at intermediate θ values could be more definitive. Detailed $B_{c2}(\theta, \phi, t)$ for the proposed f-wave forms for the C phase of UPt_3 could provide supporting information [28].

From analytic expressions for parallel-spin, p-wave superconductors with completely broken symmetry, we calculated $B_{c2}(\theta, \phi, t)$ with general ellipsoidal Fermi surface anisotropy. For Fermi surface anisotropy function $\gamma^2(\phi) > 3$, the competing effects of order parameter and Fermi surface anisotropy lead to a novel, non-monotonic θ dependence that can provide a definitive test of order parameter symmetry in URhGe. Our technique can generally provide accurate bulk tests of order parameter orbital symmetry for unconventional superconductors, provided that $V_{\sigma,\sigma'}(\hat{\boldsymbol{k}}, \hat{\boldsymbol{k}}')$ and when necessary, Pauli-limiting interactions, are appropriately transformed.

The authors thank A. D. Huxley and K. Scharnberg for useful discussions. This work was supported in part by the Florida Education Fund, the McKnight Doctoral Fellowship, the Specialized Research Fund for the Doctoral Program of Higher Education of China (no. 20100006110021) and by Grant no. 11274039 from the National Natural Science Foundation of China.

[1] N. T. Huy *et al.*, Phys. Rev. Lett. **99**, 067006 (2007).
[2] A. de Visser *et al.*, Phys. Rev. Lett. **102**, 167003 (2009).
[3] D. Aoki *et al.*, Nature **413**, 613 (2001).
[4] F. Hardy and A. D. Huxley, Phys. Rev. Lett. **94**, 247006 (2005).
[5] F. Lévy, I. Sheikin, and A. Huxley, Nat. Phys. **3**, 460 (2007).
[6] E. A. Yelland *et al.*, Nature. Phys. **7**, 890 (2011).
[7] F. Lévy *et al.*, J. Phys.: Condens. Matter **21**, 164211 (2009).
[8] V. P. Mineev, C. R. Physique **7**, 35 (2006).
[9] M. Daviš *et al.*, J. Alloys Comp. **337**, 48 (2002).
[10] A. B. Shick, Phys. Rev. B. **65**, 180509(R) (2002).
[11] W. Mueller, V. H. Tran, and M. Richter, Phys. Rev. B **80**, 195108 (2009).
[12] K. Scharnberg and R. A. Klemm, Phys. Rev. B **22**, 5233 (1980).
[13] K. Scharnberg and R. A. Klemm, Phys. Rev. Lett. **54**, 2445 (1985).
[14] R. A. Klemm and K. Scharnberg, Phys. Rev. B **24**, 6361 (1981).
[15] G. E. Volovik and L. P. Gor'kov, Zh. Eksp. Teor. Fiz. **88**, 1412 (1985) [Sov. Phys. JETP **61**, 843 (1985)]
[16] E. I. Blount, Phys. Rev. B **32**, 2935 (1985).
[17] J. Sauls, Adv. Phys. **43**, 113 (1994).
[18] V. P. Mineev and K. V. Samokhin, *Introduction to Unconventional Superconductivity* (New York: Gordon and Breach 1999).
[19] R. A. Klemm, *Layered Superconductors Volume 1* (Oxford University Press, Oxford, UK and New York, NY 2012).
[20] R. A. Klemm and J. R. Clem, Phys. Rev. B **21**, 1868 (1980).
[21] M. Prohammer and J. P. Carbotte, Phys. Rev. B **42**, 2032 (1990).
[22] E. Helfand and N. R. Werthamer, Phys. Rev. **147**, 288 (1966).
[23] C. T. Rieck and K. Scharnberg, Physica B **163**, 670 (1990).
[24] A. P. Mackenzie and Y. Maeno, Rev. Mod. Phys. **75**, 6547 (2003).
[25] S. Kittaka *et al.*, Phys. Rev. B **80**, 174514 (2009).
[26] K. Machida and M. Ichioka, Phys. Rev. B **77**, 184515 (2008).
[27] H. A. Vieyra *et al.*, Phys. Rev. Lett. **106**, 207001 (2011).
[28] Y. Machida *et al.*, Phys. Rev. Lett. **108**, 157002 (2012).